ELSEVIER

Journal of Molecular Catalysis A: Chemical 145 (1999) 273–280

JOURNAL OF MOLECULAR CATALYSIS A: CHEMICAL

www.elsevier.com/locate/molcata

Dehydrogenation of alcohols over potassium zinc aluminum silicate hydroxide

Keiji Hashimoto *, Naoji Toukai

Osaka Municipal Technical Research Institute, Morinomiya Joto-ku Osaka, 536-8553 Japan

Received 10 August 1998; accepted 15 December 1998

Abstract

Dehydrogenation of alcohol over potassium zinc aluminum silicate hydroxide, Zn-Mica, has been studied. The Zn-Mica is highly active for the dehydrogenation, and the dehydrogenation of *sec*- and *n*-alcohol is selectively converted to ketones and aldehydes, respectively. NH_3 and CO_2-TPD show that the mica is an acid–base bifunctional catalyst. FTIR measurements indicate the presence of carboxylate ions adsorbed on Zn-Mica during the dehydrogenation of *n*- and *sec*-propanol. These results indicate that the dehydrogenation proceeds via a carboxyl intermediate which is formed by adsorption of *n*- and *sec*-propanol on oxygen bridged with Zn.

Keywords: Dehydrogenation; Mica; Acetone; Base catalyst

1. Introduction

Dehydrogenation of alcohols is well known as a base-catalyzed reaction [1–9]. The dehydrogenation results in numerous, large-volume chemicals such as acetone, propanal and butanal which are valuable solvents and/or law materials of surfactant [10–14]. Moreover, the dehydrogenation of alcohols is useful for energy storage, because of the chemically best pumps based on propanol/acetone reaction [15–19]. The dehydrogenation of alcohols frequently accompanies with its dehydration to a corresponding olefin, and so the selective dehydrogenation is of great importance for practice use. In addition, these reactions will prove of great use as a test reaction of a base-catalyst.

The interlayer regions of micas have been noticed as a unique reaction field, because some interaction effects of layer charge, hydrogen bonding on intercalated molecules and/or steric effect are available to improve a synthesis of organic compounds. Potassium zinc aluminosilicate hydroxide, $K^+[Zn_3(Si_3Al)O_{10}(OH)_2]^-$, has a structure similar to that of mica: aluminum ions of phlogopite are replaced by zinc ions and the replacement gives potassium zinc aluminosilicate hydroxide, the structure of which is shown in Fig. 1. Hence the interlayer regions should be effective for organic syntheses, as expected. In addition the replacement of aluminum ions with zinc ions should improve acidic

* Corresponding author. Tel.: +81-6963-8031; Fax: +81-6963-8040; E-mail: hasimoto@omtri.city.osaka.jp

1381-1169/99/$ - see front matter
PII: S1381-1169(99)00018-7

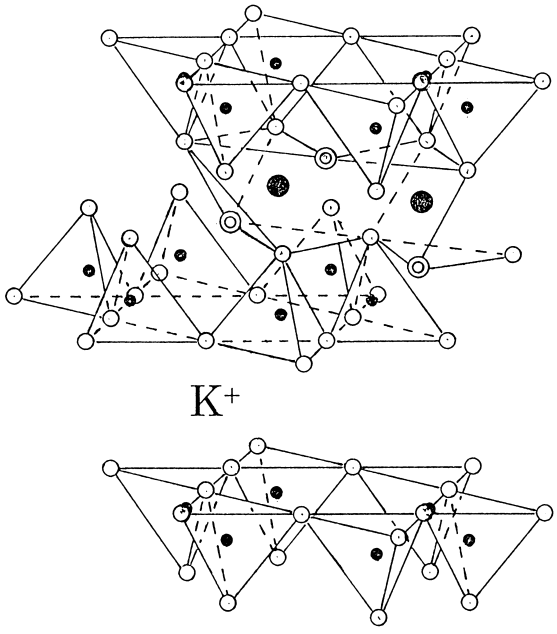

Fig. 1. Schematic representation of a structure of potassium zinc aluminum silicate hydroxide. Open circles are O^{2-}. Double circles are OH^-. Big dark circles are Zn^{2+}. Small dark circles are Al^{3+} or Si^{4+}. In potassium zinc aluminum silicate hydroxide, which has an idealized anhydrous unit cell composition of $K^+[Zn_3(AlSi_3)O_{10}(OH_2)^-]$, Al^{3+} and Si^{4+} occupied the upper and lower layers of tetrahedral holes, Zn^{2+} occupies the central layer of octahedral holes, and K^+ is the interlayer exchange cation. d_{001} defines the 001 basal spacing.

property of mica and appear as a basic one. Potassium zinc aluminum silicate hydroxide must be expected to apply to a base-catalyzed reaction. Therefore we attempted to apply potassium zinc aluminum silicate hydroxide to dehydrogenation of *sec*-propanol, *n*-propanol, and *n*-butanol. In this paper we report the (1) dehydrogenation of *sec*-propanol, (2) dehydrogenation of *n*-propanol and *n*-butanol, (3) basic property of Zn-Mica, (4) acidic property of Zn-Mica, and (5) dehydrogenation mechanism.

2. Experimental

2.1. Materials

All chemicals used were commercial materials of analytical grade and used without further purification. Colloidal silica containing 18 wt.% of SiO_2 and less than 0.5 wt.% of sodium (Nissan Chemical Industry) was used without further purification; its commercial name is Snowtex N.

2.2. Preparation of potassium zinc aluminum silicate hydroxide, Zn-Mica

Potassium hydroxide, 310 g (5.5 moles), was dissolved in 500 ml of deionized water. Aluminum nitrate hydrate, 65.0 g (0.175 moles), and zinc nitrate hydrate, 180.0 g (0.605 moles), were dissolved in 400 ml of deionized water. The solution of aluminum and zinc nitrate was then added to the potassium hydroxide solution, and a transparent mixture of aluminum and zinc hydroxides to be soluble in potassium hydroxide solution was obtained. The transparent solution was added to the colloidal silica, 220 g, containing 0.66 moles of SiO_2 and the resulting sol was allowed to age overnight. The solution took place in 2 l of an autoclave and crystallized at 150°C for a week. The resulting slurry of mica crystalline was filtered, washed several times with deionized water, and dried at 150°C for 3 h. The BET surface area of the Zn-Mica is 41 m^2/g. The chemical components are analyzed using an Inductively Coupled Plasma method (ICP) and summarized in Table 1.

2.3. Dehydrogenation of secondary-alcohol to ketones

Reactions were carried out at 250–350°C in a pulse microcatalytic reactor which was made of a stainless reaction tube of a 1-mm inner diame-

Table 1
Chemical composition of the catalyst

Catalyst	Composition (wt.%)			
	K	Al	Zn	Si
Zn-Mica	7.1	4.9	35	15
	7.2[a]	5.0[a]	36.3[a]	15.6[a]

[a] Value calculated from the formula, $K^+[Zn_3(Si_3Al)O_{10}(OH)_2]^-$.

ter. A catalyst (0.010 g) was sandwiched with quartz wool in the pulse microcatalytic reactor. The catalyst was heated for 2 h at 300°C under a carrier gas prior to the reaction. The microcatalytic reactor was cooled to a fixed reaction temperature and a pulse of 0.1–1.8 μl of *sec*-propanol was injected to the catalyst bed. The injection of *sec*-propanol was carried out three times every amount of the pulse at each reaction temperature to check the stability of the catalytic activity. The reaction temperature was raised at intervals of 20° and 30° from 250° to 350°C and then lowered in inverse order. Helium at a flow rate of 12 ml/min was used as the carrier gas. The reaction products were analyzed on-line by gas chromatography. Quartz wool (packing materials) and stainless tube do not contribute to the reaction under these conditions.

2.4. Dehydrogenation of normal-alcohol to aldehyde

The conversion of *n*-propanol or *n*-butanol was also carried out at 280–340°C in the pulse microcatalytic reactor. The weight of used catalyst was the same as that in the dehydrogenation of *sec*-propanol and pretreated for 2 h at 300°C and the same flow rate, 12 ml/ml, of helium carrier gas. The other reaction conditions were the same as those described above and their products were analyzed by the same method. The stainless tube and quartz wool scarcely contribute to the reaction under these conditions.

2.5. X-ray powder diffraction (XRD)

XRD patterns of the samples were recorded using a McScience XP_{18} spectrometer (Ni-filtered CuKα, 40 kV-50 mA). The sample was mounted on a sample board and the measurements were immediately performed. XRD peak positions were corrected using the peak resulting from Si powder as calibrator.

2.6. FTIR Measurement

FTIR spectra were recorded on a Shimadzu FTIR 8100 using a conventional IR cell connected to a vacuum line and adsorption apparatus. The sample (0.01 g) was pressed at 7.5 tons/cm^2 using a pellet die to form a wafer with a 10-mm diameter and placed into the in situ IR cell allowing heating under a vacuum. After the wafer was heated in vacuo for 1 h, the wafer was exposed to *sec*-propanol vapor (2 kPa) at a fixed temperature for 10 min. FTIR spectra of adsorbed *sec*-propanol were then recorded at room temperature.

2.7. CO_2-temperature programmed desorption (CO_2-TPD)

CO_2-TPD measurements were recorded using a Cahn Electrobalance system 2000. Potassium zinc aluminosilicate dihydroxide, about 70 mg, was exactly weighted and evacuated at 300°C till the weight of the Zn-Mica became a constant which was used as a base weight. The Zn-Mica was then exposed to CO_2 at 25°C and 1.8 kPa of CO_2 pressure. After the adsorption equilibrium was attained, carbon dioxide was evacuated at 25°C till the sample weight became a constant. The sample was then heated in vacuo at 3°C/min up to 300°C. An amount of irreversible adsorption of carbon dioxide was determined by excess weight above the base value.

2.8. NH_3-temperature programmed desorption (NH_3-TPD)

NH_3-TPD was carried out using the same apparatus as that in the CO_2-TPD. The Zn-Mica, about 70 mg, was exactly weighted and pretreated by the same procedure as that in CO_2-TPD. The sample was then exposed to NH_3 at 100°C and 1.2 kPa of NH_3 pressure. After the adsorption equilibrium was attained, NH_3 was evacuated at 100°C till the weight of the adsorbed sample became a constant. The sample

was then heated in vacuo at 3°C/min up to 300°C. An amount of the irreversible adsorption of NH_3 was also determined by excess weight above the base value.

3. Results and discussions

Dehydrogenation of *sec*-propanol over Zn-Mica was studied and the results were summarized in Table 2. The dehydrogenation selectively gives acetone at 250°C whereas the dehydration of *sec*-propanol to propene proceeds slightly at 280°C, and increases with an increase in reaction temperature and the amount of pulsed alcohol. No aldol condensation of acetone occurs even at 350°C.

Dehydrogenation of *n*-propanol and *n*-butanol over Zn-Mica was studied and the results were summarized in Tables 3 and 4. If the reaction conditions are identical, the conversion is proportional to the dehydrogenation rate. In the experiments numbers of 5 in Table 2 and 2 in Tables 3 and 4, the amount of pulsed alcohol is 0.4 μl and the other reaction conditions are also the same. The dehydrogenation rate of *n*-propanol is slower than that of *n*-butanol. The dehydrogenation rate increases in the following order: *n*-propanol < *n*-butanol < *sec*-propanol. This reactivity is independent of the molecular size of alcohol. The rate controlling step of the dehydrogenation hence is not diffusion. In the literature [20], the bond dissociation energy of O–H group is 418, 423, and 431 kJ mol^{-1} in *sec*-propanol, *n*-propanol, and *n*-butanol, respectively. The order of the dehydrogenation rate is different from that of the bond dissociation energy of O–H in alcohol. This fact strongly suggests that the rate controlling step of the

Table 2
Dehydrogenation of *sec*-propanol to acetone

No.	Temp. (°C)	Pulse[a] (μl)	Conv. (mol%)	Acetone (mol%)	Selectivity (%)
1	250	0.1	37.8	37.8	100
2	250	0.4	23.1	23.1	100
3	250	1.0	10.4	10.4	100
4	280	0.05	84.8	82.0	96.7
5	280	0.4	58.2	55.4	95.2
6	280	0.5	51.5	49.0	95.1
7	280	1.0	29.7	28.2	94.9
8	300	0.4	100	94.8	94.8
9	300	0.6	85.2	81.1	95.2
10	300	1.2	55.3	51.9	93.9
11	330	0.5	100	94.7	94.7
12	330	1.0	100	90.5	90.5
13	350	0.2	100	94.3	94.3
14	350	0.8	100	91.1	91.1
15	350	1.8	84.2	78.8	93.6

[a]The amount of pulsed *sec*-propanol. Catalyst: 0.010 g. Flow rate of He: 12 ml/min.

Table 3
Dehydrogenation of *n*-propanol to *n*-propanal

No.	Temp. (°C)	Pulse[a] (μl)	Conv. (mol%)	Propanal (mol%)	Selectivity (%)
1	280	0.6	6.2	6.2	100
2	280	0.4	9.2	9.2	100
3	300	0.2	35.2	35.2	100
4	300	0.05	39.8	39.8	100
5	320	0.7	25.0	23.2	92.8
6	320	0.6	29.2	26.9	92.1
7	340	1.0	23.7	21.5	90.7
8	340	0.9[b]	32.8	24.4	74.4

[a]The amount of pulsed *n*-propanol. Catalyst: 0.010 g. Flow rate of He: 12 ml/min.
[b]Flow rate of He, 10 ml/min.

Table 4
Dehydrogenation of *n*-butanol to *n*-butanal

No.	Temp. (°C)	Pulse[a] (μl)	Conv. (mol%)	Butanal (mol%)	Selectivity (%)
1	280	0.5	9.4	9.4	100
2	280	0.4	15.4	15.4	100
3	280	0.05	35.9	35.9	100
4	300	0.4	29.6	29.6	100
5	300	0.3	40.1	40.1	100
6	320	0.5	29.9	29.9	100
7	320	0.4	50.1	50.1	100
8	320	0.3	56.3	56.3	100
9	340	0.6	39.4	39.4	100
10	340	0.5	55.0	55.0	100
12	340	0.4	69.2	69.2	100

[a]The amount of pulsed *n*-butanol. Catalyst: 0.010 g. Flow rate of He: 12 ml/min.

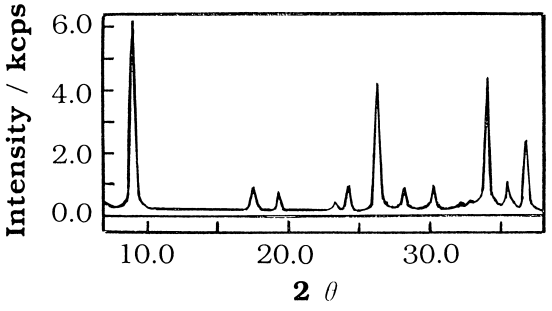

Fig. 2. X-ray powder diffraction patterns.

dehydrogenation is not the breaking of the OH bond. Dehydrogenation of *n*-propanol and *n*-butanol selectively gives a corresponding aldehyde at temperature up to 300°C, whereas dehydration of *n*-propanol to propene and aldol condensation of produced propanal proceed slightly above 300°C; the main product of *n*-propanol dehydration is propene and dipropyl ether is negligible. The product due to aldol condensation at 340°C is 2.1 and 6.4 mol% of the products in the experiments numbers of 7 and 8 in Table 3, respectively. These results indicate that a bimolecular reaction hardly occurs at a temperature below 300°C, whereas slightly increases at 300–340°C.

X-ray powder diffraction patterns were recorded and shown in Fig. 2. The patterns well agree with those for potassium zinc aluminum silicate hydroxide in the literature [21]. The space distance, $d(0,0,1)$, and *b*-parameter are hence determined to be 1.02 nm and 0.924 nm, respectively. The layer consists of two aluminosilicate sheets and one zinc oxide sheet. A sum of an aluminosilicate sheet thickness and a zinc oxide sheet one which is capable of a replacement with a diameter of O^{2-}, 0.24 nm, is $1/2$ of *b*-parameter. The thickness of the layer is calculated to be 0.68 nm$\fallingdotseq 2(0.462-0.24) + 0.24$. The distance of the interlamellar space is calculated to be 0.34 nm = 1.02–0.68. *sec*-Propanol is capable of intercalation in the interlamellar space of Zn-Mica, because the minimum width, 0.24 nm, of its molecule is smaller than the distance of the interlamellar space: the minimum width of an optimized *sec*-propanol molecule is computed to be 0.242 nm using a usual MM2 method (Cambridge-Soft). The crystal size of the Zn-Mica was determined to be 29 nm from the half width of the peaks at (1,0,0), and (3,0,0), and 37 nm from that at (1,3,1) and (1,3,2), using Scherrer's equation [22].

FTIR spectra of Zn-Mica were recorded and shown in Figs. 3 and 4. The isopropyl group gives rise to a moderately strong band in the 3000–2840 cm^{-1} region [23] and a liquid *sec*-propanol gives three bands at 2973, 2934 and 2884 cm^{-1}; asymmetric stretching vibration of $-CH_3$ appears at $\sim$2960 cm^{-1}, symmetric one of $-CH_3$ at $\sim$2870 cm^{-1} and stretching vibration of C–H bond in –CH(OH)– group of *sec*-propanol at 2934 cm^{-1}. As shown in Fig. 3b, the adsorption of *sec*-propanol at 250°C on Zn-Mica gives the bands at 2969, 2877, and 2927 cm^{-1} which are attributed to the stretching vibrations of $-CH_3$ and C–H in –CH(OH)–

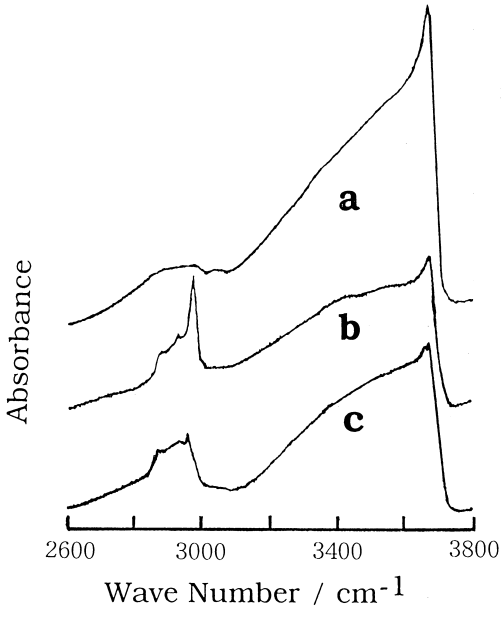

Fig. 3. IR spectra of adsorbed *sec*-propanol and acetone. (a) Evacuation for 2 h at 400°C. (b) Exposure at 250°C for 10 min to 2.0 kPa of *sec*-propanol vapor after the evacuation. (c) Exposure at 250°C for 10 min to 2.0 kPa of acetone vapor after the evacuation.

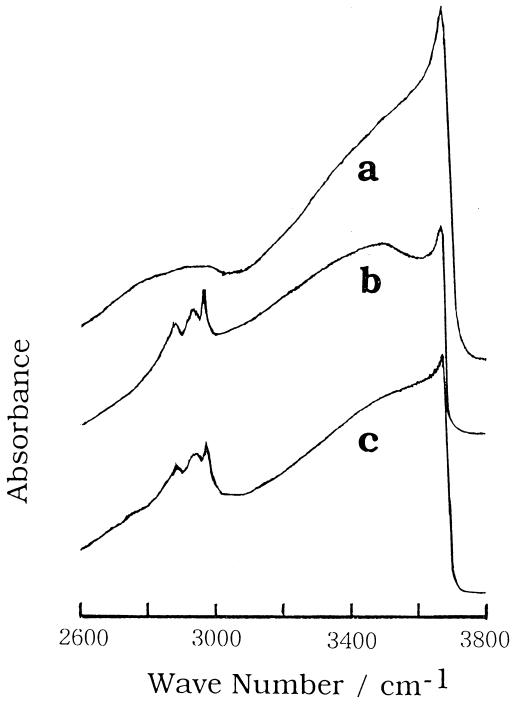

Fig. 4. IR spectra of adsorbed *n*-propanol and propanal. (a) Evacuation for 2 h at 400°C. (b) Exposure at 280°C for 10 min to 2.0 kPa of *n*-propanol vapor after the evacuation. (c) Exposure at 280°C for 10 min to 2.0 kPa of propanal vapor after the evacuation.

group. On adsorbing, the stretching vibrations shift from 2973, 2934 and 2884 cm^{-1} to 2969, 2927 and 2877 cm^{-1} respectively. Moreover, the adsorption decreases the intensity of the band at 3667 cm^{-1} assigned to the O–H stretching vibration of free hydroxyl group. This result strongly suggests the adsorption of *sec*-propanol on the free hydroxyl group as isopropyl ether bonding. As shown in Fig. 5d and e, the adsorption of *sec*-propanol and acetone at 250°C gives the bands at 1717 and 1578 cm^{-1}. The band at 1717 cm^{-1} is attributed to the stretching vibration of the carbonyl group [23], and this appearance indicates the formation of acetone. The band at 1578 cm^{-1} is attributed to the stretching vibration of carboxylate ion [3,23]. This result indicates that the carboxylate ion is an intermediate of the dehydrogenation and attached to zinc oxide and/or aluminosilicate in the Zn-Mica framework. A similar intermediate has been observed in the adsorption of alcohol on a basic metal oxide and acid–base amphoteric one [2,3,24,25].

The adsorption of *n*-propanol on Zn-Mica gives the bands at 2965, 2940 and 2882 cm^{-1} as shown in Fig. 4b, and are attributed to the stretching vibrations of methyl and methylene group [23]; asymmetric stretching vibration of $-CH_3$ appears at $\sim$2960 cm^{-1}, symmetric one of $-CH_3$ at $\sim$2870 cm^{-1} and asymmetric one of $-CH_2-$ at $\sim$2940 cm^{-1}. The adsorption shifts the bands from 2963, 2938 and 2878 to 2965, 2936 and 2882 cm^{-1}. The intensity of the band at 3667 cm^{-1} decreases on adsorbing *n*-propanol. The result also suggests the adsorption of *n*-propanol on the free hydroxyl group. As shown in Fig. 5b and c, the strong band at 1574 cm^{-1} appears, when adsorbing *n*-propanol and *n*-propanal, and is attributed to the stretch-

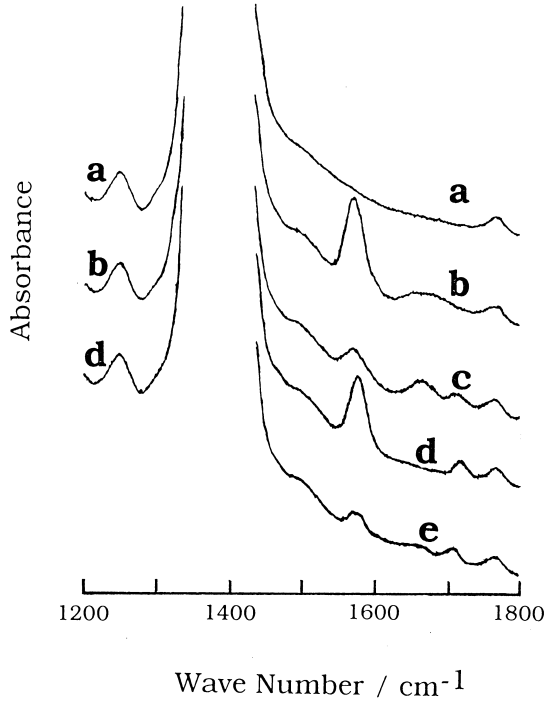

Fig. 5. IR spectra of adsorbed reaction intermediates. (a) Evacuation for 2 h at 400°C. (b) Exposure at 280°C for 10 min to 2.0 kPa of *n*-propanol vapor. (c) Exposure at 280°C for 10 min to 2.0 kPa of propanal vapor. (d) Exposure at 250°C for 10 min to 2.0 kPa of *sec*-propanol vapor. (e) Exposure at 250°C for 10 min to 2.0 kPa of acetone vapor.

ing vibration of carboxylate ion. This result also indicates the carboxylate ion to be intermediate in the dehydrogenation of *n*-propanol. These adsorbed carboxylate ions are considered to be rather stable and suggest that the rate controlling step is a desorption of the carboxylate ion or an elimination of hydrogen from its α-carbon. The weak band around 1700 cm^{-1} is attributable to the C=O stretching vibration of propanal. The band intensity at 1250 cm^{-1} scarcely changes with the treatment temperature of the catalyst in vacuo up to 400°C. The band at 1250 cm^{-1} is attributable to the bending vibration of hydroxyl groups which consists in the Zn-Mica layer framework, as illustrated in double circles in Fig. 1. The adsorption of *n*- and *sec*-propanol has little effect on the band intensity and the bending vibration of the hydroxyl groups as shown in Fig. 5. The result indicates that the hydroxyl groups in the Zn-Mica framework scarcely contribute to the dehydrogenation.

NH_3-TPD was studied and the results were shown in Table 5. The results indicate the presence of week acid sites in the Zn-Mica. The acid sites hardly contribute to the dehydration of *n*-propanol and *n*-butanol at a temperature less than 320°C, because no dehydration is observed. As shown in Fig. 1, the layer component of Zn-Mica consists of two aluminosilicate sheets and one zinc oxide sheet, and its zinc oxide is sandwiched between two sheets of the aluminosilicate. The aluminosilicate thus exposes to the interlayer surface and so the acid sites are explainable by the presence of the surface aluminosilicate; it is well known that acidic properties are present in aluminosilicates which have exchangeable cations.

Table 5
Amount of carbon dioxide irreversibly adsorbed on Zn-Mica

Adsorption temp. (°C)	CO_2 (mg/g cat)
25	1.48
50	1.29
70	0.75
100	0.0

Table 6
Amount of NH_3 irreversibly adsorbed on Zn-Mica

Adsorption temp. (°C)	NH_3 (mg/g cat)
50	1.75
70	1.22
100	0.53
150	0.0

Dehydrogenation of alcohols is well known to be a base-catalyst reaction. CO_2-TPD was studied and the results are shown in Table 6. The results indicate the presence of basic sites. Though the Zn-Mica having both acidic and basic sites can be considered as acid–base bifunctional catalysts, the dehydrogenation due to the basic sites is thus preferred to the dehydration due to the acid sites. The number of basic sites which can form the bonding at 25°C with CO_2 are determined to be 2.0×10^{19} ($0.00148 \div 44 \times 6.022 \times 10^{23}$) sites/g cat from the irreversible adsorption of CO_2 in Table 6. The basic sites in Zn-Mica are considered to be potassium ions and/or zinc oxide: though the zinc oxide is sandwiched between two aluminosilicate sheets, a hexagonal basin like a pan is present in the aluminosilicate sheet as shown in Fig. 1 and expose the zinc oxide in its bottom. The caliber and depth of the hexagonal basin are 0.52 and 0.22 nm (thickness of aluminosilicate sheet), respectively. The sum of a distance between oxygen of a hydroxyl group and α-carbon and covalent bond radius of their atoms is 0.383 nm in *sec*-propanol, and a bond length between oxygen and carbon in C–OH group is 0.143 nm: the optimized distance and bond length were computed using the same MM2 method as described above. These facts indicate that oxygen of a hydroxyl group, one of α-carbons and carbon attaching a hydroxyl group fit in the basin, though another α-carbon rather protrudes. The formation of the carboxylate structure hence leads us to the conclusion that the bottom zinc oxide contributes to the

dehydrogenation, because the carboxylate structure are formed by an attachment of alkoxy ion with oxygen, O^{2-}, of the zinc oxide. The carboxylate ion also fits in the hexagonal basin of which periphery consists of aluminosilicate to induce acidic sites and is isolated. The alcohol molecule and the carboxylate ion attaching to the basin bottom are inevitably close to the basin periphery. Therefore, these conformations strongly suggest a synergistic effect of the acid and base sites on the dehydrogenation. The difficulty of bimolecular reaction such as a formation of ethers and aldol condensation is reasonably explained in terms of the isolated conformation of the carboxylate ion and alcohol in the basin.

4. Conclusion

Dehydrogenation of *n*-propanol, *n*-butanol and *sec*-propanol over the Zn-Mica is selectively convertible to a corresponding aldehyde and acetone. Both of ammonia and CO_2 are irreversibly adsorbed on the Zn-Mica and so the Zn-Mica is an acid–base bifunctional catalyst. However, the dehydrogenation due to its basic sites is preferred to the dehydration due to its acidic sites. The adsorption of *sec*-propanol or acetone on the Zn-Mica gives carboxylate ions. On adsorbing alcohol, oxygen of hydroxyl group, α-carbon and carbon attaching to a hydroxyl group fit in the hexagonal basin, which consists of aluminosilicate to induce acidic sites, and the isolated alcohol is inevitably close to the basin periphery. It is hence concluded that the dehydrogenation proceeds via an intermediate of the carboxylate ions attaching to the bottom zinc oxide. The conformation strongly suggests a synergistic effect of the acid and base sites on the dehydrogenation. Therefore, Zn-Mica is a useful acid–base bifunctional catalyst.

References

[1] H. Niiyama, E. Echigoya, Bull. Chem. Soc. Jpn. 44 (1971) 1739.
[2] L. Nondek, J. Sedlácêk, J. Catal. 40 (1975) 34.
[3] N. Takezawa, C. Hanamaki, H. Kobayashi, J. Catal. 38 (1975) 101.
[4] M. Akimoto, Shokubai Kouza 8, Catalysis Society of Japan, 1985, 235 pp.
[5] A.R. Davydova, T.M. Yuréva, T.P. Minyukova, M.P. Demeshkina, Aktual. Probl. Proizvod. katal, Prom. Katal., Tr. Semin., 2nd, 1994, 2, p. 149.
[6] A. Corma, V. Fornés, F. Rey, J. Catal. 148 (1994) 205.
[7] A. Music, J. Batista, J. Levec, Appl. Catal. A 165 (1–2) (1997) 115.
[8] E.J. Doskocil, S.V. Bordawekar, R.J. Davis, J. Catal. 169 (1) (1997) 327.
[9] S.V. Bordawekar, E.J. Doskocil, R.J. Davis, Catal. Lett. 44 (3,4) (1997) 193.
[10] K. Schmitt, Chem. Ind. 18 (1966) 204.
[11] W.T. Reichle, J. Catal. 63 (1980) 295.
[12] B. Burczyk, Tenside Detergents 17 (1980) 21.
[13] L. Weclas, Tenside Detergents 18 (1981) 19.
[14] C.H. Richard, F.J. Albert, J. Am. Oil Chem. Soc. Inform 7 (1996) 428.
[15] Y. Saitou, Hydrogen Energy Prog., 11th Proc. World Hydrogen Energy Conf., 1996, 2, p. 2011.
[16] T. Cunningham, J.N. Hickey, Z. Wang, Int. J. Energy Res. 20 (9) (1996) 763.
[17] S. Kajima, T. Kajita, H. Furuta, Jpn. Kokai Tokkyo Koho JP 09,268,144 [97,268,144].
[18] J. Chen, Avail. UMI, Order No.DA9737397; CA., 128, 8666d (1997).
[19] Y. Ohko, A. Fujiwara, K. Hashimoto, J. Phys. Chem. B 102 (10) (1998) 1724.
[20] The Chemical Society of Japan, Kagakubinran Kisohen, 2nd edn., Maruzen Press, 1975, p. 977.
[21] A.J. Perrotta, T.J. Garland, Am. Mineral. 60 (1975) 152.
[22] P. Scherrer, Göttinger Nachrichten 2 (1918) 98.
[23] R.M. Silberstein, G.C. Bassler, Spectrometric Identification of Organic Compounds, Wiley, 1963, p. 56.
[24] A.A. Davydov, V.M. Shchekochikhin, P.M. Zaitsev, I.M. Shchekochikhin, N.P. Keier, Kinet Katal. 12 (1971) 694.
[25] H. Bohlbro, An Investigation on the Kinetics of the Conversion of Carbon Monoxide with Water Vapor over Iron Oxide Based Catalysts, 2nd edn., Gjellerup, Copenhagen, 1969.